

# Microparticles initiate decompression-induced neutrophil activation and subsequent vascular injuries

Stephen R. Thom,<sup>1,2</sup> Ming Yang,<sup>1</sup> Veena M. Bhopale,<sup>1</sup> Shaohui Huang,<sup>1</sup> and Tatyana N. Milovanova<sup>1</sup>

<sup>1</sup>Institute for Environmental Medicine and <sup>2</sup>Department of Emergency Medicine, University of Pennsylvania Medical Center, Philadelphia, Pennsylvania

Submitted 20 July 2010; accepted in final form 14 October 2010

**Thom SR, Yang M, Bhopale VM, Huang S, Milovanova TN.** Microparticles initiate decompression-induced neutrophil activation and subsequent vascular injuries. *J Appl Physiol* 110: 340–351, 2011. First published October 21, 2010; doi:10.1152/jappphysiol.00811.2010.—Progressive elevations in circulating annexin V-coated microparticles (MPs) derived from leukocytes, erythrocytes, platelets, and endothelial cells are found in mice subjected to increasing decompression stresses. Individual MPs exhibit surface markers from multiple cells. MPs expressing platelet surface markers, in particular, interact with circulating neutrophils, causing them to degranulate and leading to further MP production. MPs can be lysed by incubation with polyethylene glycol (PEG) telomere B surfactant, and the number of circulating MPs is reduced by infusion of mice with PEG or antibody to annexin V. Myeloperoxidase deposition and neutrophil sequestration in tissues occur in response to decompression, and the pattern differs among brain, omentum, psoas, and leg skeletal muscle. Both MP abatement strategies reduce decompression-induced intravascular neutrophil activation, neutrophil sequestration, and tissue injury documented as elevations of vascular permeability and activated caspase-3. We conclude that MPs generated by decompression stresses precipitate neutrophil activation and vascular damage.

decompression sickness; intravascular bubble; leukocytes; platelets; antigen sharing; CD41; integrins; myeloperoxidase

DECOMPRESSION SICKNESS (DCS) is a systemic pathophysiological process that occurs after tissues become supersaturated with gas. Inert gases inhaled while breathing are taken up by tissues in proportion to the ambient pressure, and when pressure is reduced, some of this gas is released from tissues in the form of bubbles (12). The central role of bubbles as an inciting factor for DCS is widely accepted, but the pathophysiological responses that mediate tissue injury remain unclear. DCS has been associated with endothelial dysfunction, platelet activation, occasional alterations in coagulation pathways, and rare reduction of circulating platelet counts (6, 32–34). Neutrophil activation and perivascular adherence are associated with functional deficits after decompression in animal models (27, 31). DCS is a risk associated with scuba diving, high-altitude aviation, and space exploration.

Circulating microparticles (MPs) are increased in humans subjected to simulated scuba diving (26, 45). MPs are 0.1- to 1- $\mu$ m-diameter membrane vesicles shed from the surface of cells by what appear to be well-regulated processes (13). MPs are characterized by their expression of antigenic markers from parent cells. As MPs bud from these cells, negatively charged phosphatidylserine residues are exposed, often leading to sec-

ondary binding of annexin V. MPs can directly stimulate release of proinflammatory cytokines, and platelet-derived MPs stimulate leukocyte activation and aggregation (22, 24, 28). Annexin V-positive platelet MPs exhibit procoagulant activity (9). Testing the pathological or physiological roles of MPs has been difficult, because methods to remove circulating MPs are limited. We hypothesized that MPs generated on decompression are required for development of tissue injuries. Using novel surfactant-based and antibody infusion methods to abate circulating MPs, we show their involvement with intravascular neutrophil activation and generation of vascular injuries in mice subjected to a range of decompression stresses.

## METHODS

**Materials.** Unless otherwise noted, chemicals were purchased from Sigma-Aldrich (St. Louis, MO). Antibodies were purchased from sources as described below.

**Animals.** All aspects of this study were reviewed and approved by the Institutional Animal Care and Use Committee. Wild-type mice (*Mus musculus*) and myeloperoxidase (MPO) knockout mice were purchased from Jackson Laboratories (Bar Harbor, ME); they were fed a

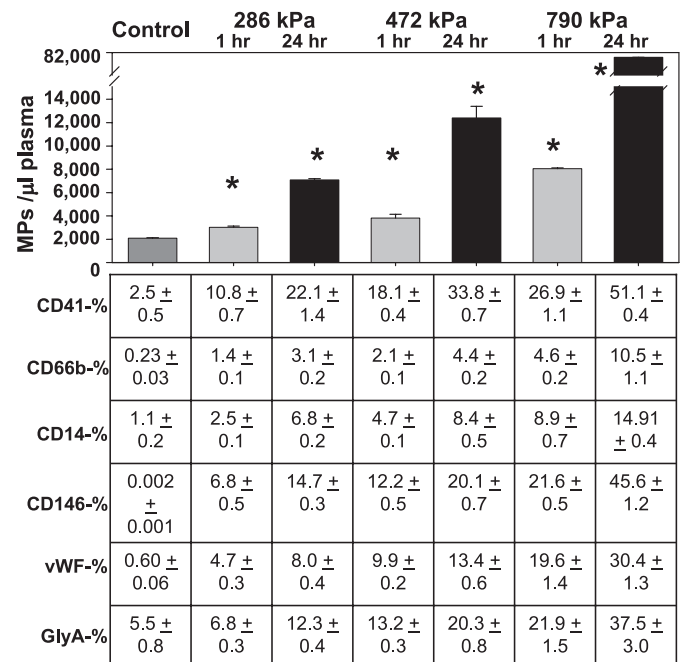


Fig. 1. Microparticle (MP) changes with decompression. *Top*: blood-borne MPs in control mice and mice killed at 1 or 24 h postdecompression. *Bottom*: fraction of MP populations that exhibit surface markers for annexin V and each of the vascular cell proteins. vWF, von Willebrand factor; GlyA, glycophorin A. Values are means  $\pm$  SE ( $n = 4$ –26 per group). All values are significantly different from control (by 2-way ANOVA). \* $P < 0.05$ .

Address for reprint requests and other correspondence: S. R. Thom, Institute for Environmental Medicine, Univ. of Pennsylvania, 1 John Morgan Bldg., 3620 Hamilton Walk, Philadelphia, PA 19104-6068 (e-mail: sthom@mail.med.upenn.edu).

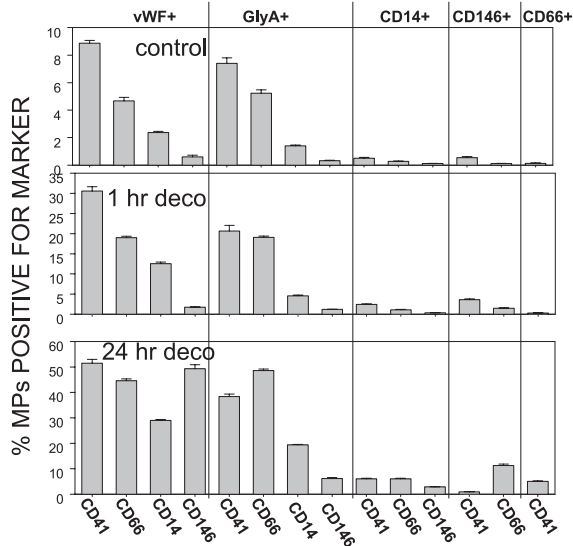


Fig. 2. MPs display multiple cell markers. MPs were stained to detect proteins from vascular cell sources. Bars show percentage of MPs expressing annexin V, the cell surface marker (*top*), and the antigen (*bottom*). Values are means  $\pm$  SE ( $n = 4-26$  per group). All values in decompression (deco) groups, except number of MPs expressing CD146 + CD41 and CD66 + CD41, are significantly different from control (by 2-way ANOVA).

standard rodent diet and water ad libitum and were housed in the animal facility of the University of Pennsylvania. A colony of MPO knockout mice was maintained from breeding pairs. Mice were exposed to elevated pressure in a small hyperbaric chamber (model G15-APSP, Bethlehem Steel). Pressurization and decompression oc-

curred at 200 kPa/min. There were no deaths due to the pressure profiles used in this study. At the times specified in RESULTS, mice were anesthetized [intraperitoneal administration of ketamine (100 mg/kg) and xylazine (10 mg/kg)], skin was prepared by swabbing with povidone-iodine (Betadine), and blood was collected in heparinized syringes by aortic puncture. Blood was immediately combined with commercial fixative (100  $\mu$ l/ml Caltag Reagent A fixation medium, Invitrogen, Carlsbad, CA) before further work was done.

Thrombocytopenia was achieved by injection of antiserum, as previously described (40). A 0.3% solution (wt/vol) of sterile polyethylene glycol (PEG) telomere B was infused at 0.7  $\mu$ l/g mouse immediately following decompression. Other mice were injected with annexin V antibody (2  $\mu$ g/g mouse iv; BD Pharmingen, San Jose, CA) immediately following decompression.

**Flow cytometry.** Flow cytometry was performed with a 4-color, dual-laser analog FACSCalibur or 10-color FACSCanto (Becton-Dickinson, San Jose, CA) using standard acquisition software. Analysis of leukocytes was performed on fixed blood. Erythrocytes were not removed to guard against cell activation that might occur with lysis steps. Assay methods, permeabilization, and compensation procedures were carried out as described in a previous publication (30). Cells were defined as positive for a particular antigen if linear fluorescence intensity was  $>10$ .

MPs were obtained from fixed blood by a three-step procedure involving an initial centrifugation at 150 g for 20 min to remove cells; then the plasma supernatant was centrifuged at 300 g for 20 min to clarify the platelet-rich plasma. EDTA was added to achieve 0.2 M, plasma was centrifuged for 30 min at 15,000 g, and the supernatant was used for MP analysis. This protocol was established on the basis of pilot trials focused on eliminating cell debris, which was expected to be elevated by decompression stresses. Centrifugation at  $<15,000$  g resulted in more debris in the supernatant (quantitatively assessed as the  $\leq 10$ -fluorescence units particles in dot plots of forward vs. side

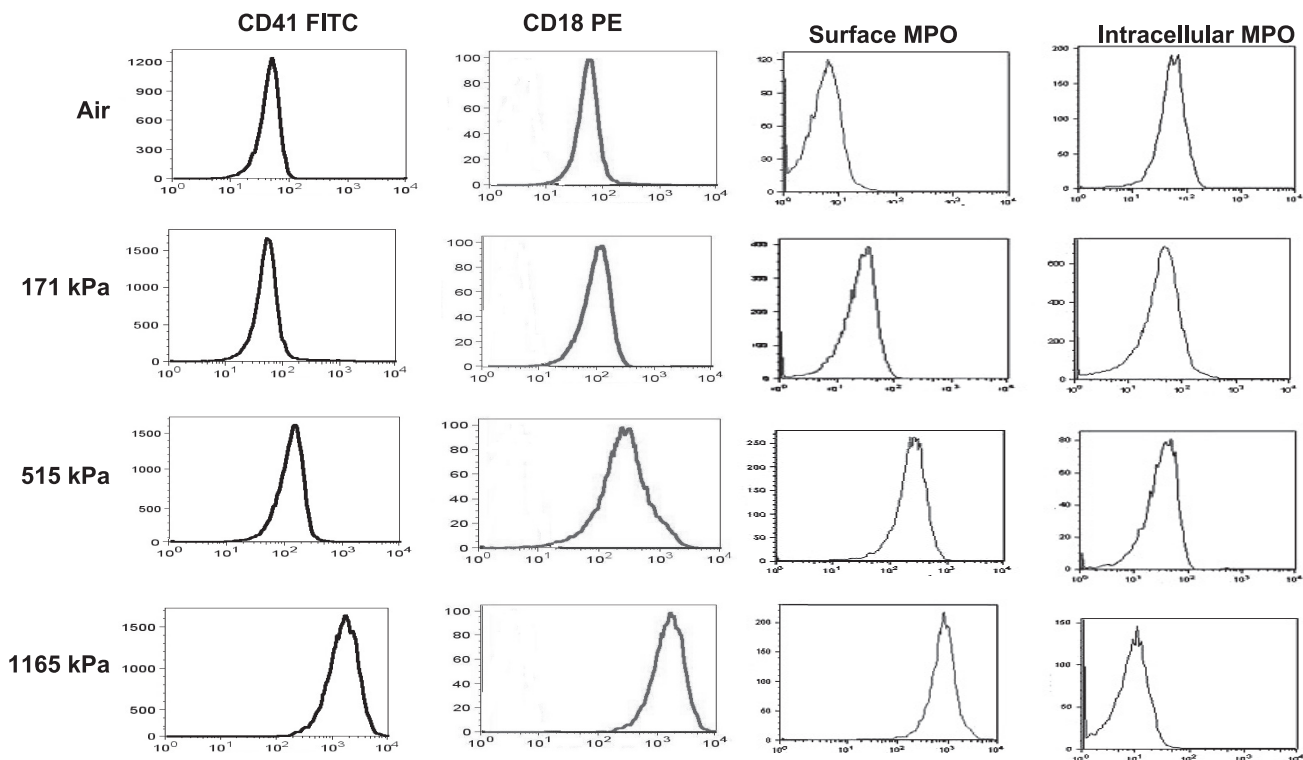


Fig. 3. Leukocyte changes with decompression. Neutrophils in blood from decompressed mice were labeled using anti-CD66b. One portion of each cell preparation was used for evaluation of surface expression of CD18, CD41, and myeloperoxidase (MPO); another portion was permeabilized and stained for evaluation of intracellular MPO content. Results from flow cytometry show surface staining and intracellular MPO in cells from mice killed immediately after decompression following exposure to 171, 515, and 1,165 kPa for 2 h.

scatter), whereas centrifugation at  $>15,000 g$  or for  $>15$  min decreased the MP counts in supernatant samples. All reagents and solutions used for MP analysis were sterile and filtered ( $0.2\text{-}\mu\text{m}$  filter).

For four-color FACSCalibur analysis, four tubes containing  $50\ \mu\text{l}$  of supernatant were mixed with  $3\ \mu\text{l}$  of annexin V-allophycocyanin (APC) conjugate (BD Pharmingen) in  $100\ \mu\text{l}$  of annexin binding buffer solution (BD Pharmingen; 1:10 vol/vol in distilled water). Additional antibodies were added to individual tubes as follows: 1)  $3\ \mu\text{l}$  of FITC-conjugated anti-mouse CD61, FITC-anti-mouse CD42, or Alexa 647-conjugated anti-lysosome-associated membrane protein-1 (LAMP-1; e-Biosciences, San Diego, CA) and  $3\ \mu\text{l}$  of R-phycoerythrin (PE)-conjugated anti-mouse CD41 (e-Biosciences), 2) FITC-conjugated anti-mouse glycoprotein A (GlyA; e-Biosciences) and PE-conjugated von Willebrand factor (vWF; BD Pharmingen), 3) FITC-conjugated anti-human CD14 (BD Pharmingen), and 4) FITC-conjugated anti-human CD66b (BD Pharmingen) and RPE-conjugated CD146 (BD Pharmingen). All tubes were incubated for 30 min in darkness prior to analysis. Gates were set to include  $\leq 1.0\text{-}\mu\text{m}$  particles, with exclusion of background corresponding to debris usually present in buffers.

For FACSCanto analysis, all antibodies (BD Pharmingen) were mouse anti-human (with cross-reaction against mouse antigens). Plasma samples ( $50\ \mu\text{l}$ ) were incubated for 30 min in darkness with  $5\ \mu\text{l}$  of FITC-conjugated anti-annexin V,  $5\ \mu\text{l}$  of RPE-conjugated anti-CD146,  $5\ \mu\text{l}$  of peridinin chlorophyll protein complex (PerCP)/Cy5.5-conjugated anti-CD41,  $5\ \mu\text{l}$  of PerCP-conjugated anti-CD66b,  $5\ \mu\text{l}$  of APC-conjugated anti-GlyA,  $5\ \mu\text{l}$  of Pacific Blue-conjugated anti-CD14, and  $5\ \mu\text{l}$  of Texas red (TR)-conjugated anti-vWF in a final volume of  $100\ \mu\text{l}$  of annexin binding buffer solution. After incubation, the sample was diluted to  $400\ \mu\text{l}$  with annexin binding buffer solution for flow cytometry analysis. Gates were set to include 0.3- to  $1.0\text{-}\mu\text{m}$  particles, with exclusion of background corresponding to debris usually present in buffers.

Analysis with both flow cytometer protocols involved establishment of true-negative controls by a fluorescence-minus-one analysis and use of isotype-matched irrelevant antibodies at the same concentration and under the same conditions. Forward and side scatter were set at logarithmic gain. Microbeads of various diameters [ $0.3\ \mu\text{m}$  (Sigma) and  $1.0$  and  $3.0\ \mu\text{m}$  (Spherotech, Lake Forest, IL)] were used for initial settings and before each experiment to measure MPs as an internal control. The absolute numbers of MPs per milliliter of plasma were determined by counting the proportion of beads and the exact volume of plasma from which MPs were analyzed.

As with other reports comparing results of FACSCanto with FACSCalibur, we found close agreement between instruments for evaluations of total number of MPs in plasma samples. However, we found large differences in measurements of MP subtypes between the two flow cytometers. Marked elevations in estimates of each MP subtype occurred with FACSCalibur vs. FACSCanto. We discerned that the discrepancy arose because  $<0.3\text{-}\mu\text{m}$  particles, although a relatively small fraction of the total, exhibited a disproportionately greater variety of surface markers from many vascular cells than did larger MPs. FACSCalibur analysis (gate set to evaluate  $\leq 1\text{-}\mu\text{m}$  particles) included  $<0.3\text{-}\mu\text{m}$  particles, contrary to the FACSCanto, where the gate could be specifically set to evaluate only 0.3- to  $1.0\text{-}\mu\text{m}$  particles. If the FACSCanto gating was enlarged to evaluate all  $\leq 1\text{-}\mu\text{m}$  particles, the MP subtype analysis matched that of the FACSCalibur. For example, we analyzed six different MP suspensions from control mice and quantified the MP subpopulation exhibiting annexin V and CD41 on the surface. The FACSCalibur measurement was  $48.8 \pm 3.5\%$  platelet-derived MPs. With the FACSCanto and with gating set to count all  $\leq 1\text{-}\mu\text{m}$  particles, the measurement was  $43.8 \pm 2.8\%$  [ $P =$  not significant (NS) vs. FACSCalibur]. If the FACSCanto was set to consider only 0.3- to  $1\text{-}\mu\text{m}$  particles, the measurement was  $3.1 \pm 0.5\%$  platelet-derived MPs ( $P < 0.05$  vs. alternate gating paradigm). Only data from subtype analyses using FACSCanto gated on 0.3- to  $1\text{-}\mu\text{m}$  particles are reported.

Control experiments were required to establish the accuracy of quantitative evaluations of MPs in mice injected with anti-annexin V antibodies ( $2\ \mu\text{g/g}$  body wt iv) to reduce circulating MP numbers. Parallel samples of blood were incubated with or without unconjugated annexin V antibody at various concentrations for 30 min before samples were processed, and MPs were stained following the protocol described above using APC-conjugated annexin V antibody. We estimated that mice were injected with  $\sim 30\ \mu\text{g}$  antibody/1 ml blood as a MP abatement strategy, so blood was incubated with unconjugated annexin V antibody at  $30\text{--}120\ \mu\text{g/ml}$ . Antibody concentrations even fourfold higher than that used in vivo did not alter total or subtype MP count estimates. For example, in four trials, the MP assessment with  $120\ \mu\text{g/ml}$  anti-annexin V in the suspension differed from a control suspension containing only PBS by  $-0.52 \pm 0.37\%$  ( $P =$  NS). Hence, we conclude that the dose of unconjugated anti-annexin V antibody used in mice was insufficient to saturate MP surface epitopes for annexin V.

**Solid-phase immunoassay.** After blood was removed from anesthetized animals, a thoracotomy was performed, the left heart was cannulated, and the right heart was opened to release perfusate. Residual blood was removed by perfusion of the mouse with  $3\text{--}4$  ml of  $20\ \text{mM}$  2-(N-morpholino)ethanesulfonic acid (MES) and  $125\ \text{mM}$  NaCl, pH 6.2 (MBS), containing  $30\ \mu\text{M}$  freshly prepared nitroprusside (as a vasodilator) and  $200\ \text{U}$  of heparin over 5 min. Tissues (brain, a hindleg skeletal muscle, psoas, and omentum) were removed, placed in  $20\ \text{mM}$  MES,  $140\ \text{mM}$  sorbitol, pH 5.0, and protease

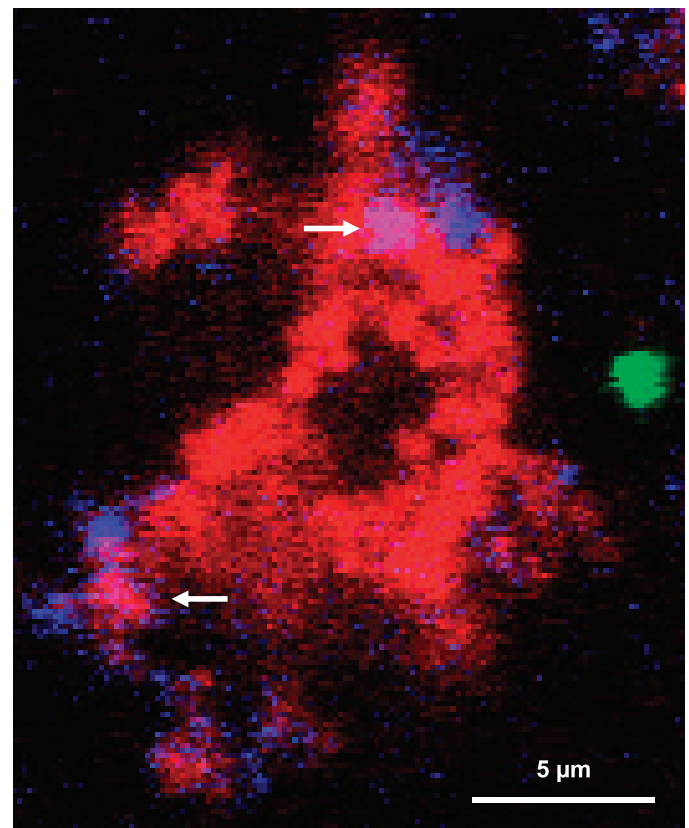


Fig. 4. Particles in blood. Representative confocal microscope image of MP particles and a neutrophil from a mouse killed 1 h after decompression from  $790\ \text{kPa}$  for 2 h. Blue CD41-positive particles, a neutrophil (CD66b, stained red), and a green  $1\text{-}\mu\text{m}$  bead are shown. The  $0.7\text{-}\mu\text{m}$ -thick confocal image was chosen to highlight MP overlap with the neutrophil (stained purple, arrows); much of the cell membrane was not in the in-focus plane. Apparent size and clarity of beads are influenced by axial position in fluid and mobility during image acquisition.

inhibitor cocktail at 1 g tissue/10 ml, minced with a razor blade in a plastic dish at 4°C, and then broken up with a Teflon pestle using 10 up-and-down strokes at 1,500 rpm. Homogenates were filtered using 50- $\mu$ m nylon mesh and centrifuged at 500 g for 10 min, protein concentration was measured, and samples were combined with 2 $\times$  SDS buffer. Adequate samples were spotted on nitrocellulose to give 1, 5, 10, and 20  $\mu$ g of protein per spot in triplicate and dried. Background fluorescence was determined and subtracted from fluorescence measured after staining with the desired fluorochrome-conjugated antibodies. Blood (1–10  $\mu$ l) from each animal was also spotted onto the individual nitrocellulose papers to allow for contaminating blood corrections. Homogenate samples were routinely assayed for residual blood following our published technique (41), and appropriate corrections were applied to calculate sequestered neutro-

phils (CD66b antibody staining) and MPO. Contamination was slight:  $0.27 \pm 0.08$  (SE)  $\mu$ l blood/100  $\mu$ l tissue homogenate ( $n = 126$ ).

**Colloidal silica-endothelium isolation technique.** Methods were modified from those described by Arjunan et al. (1). Animals were prepared as described above; after blood was removed, the animals were perfused at 0.5 ml/min for 30 min with a 1% solution of colloidal silica that had been given a positive charge by coating with aluminum chlorohydroxide and suspended in MES-saline at pH 5.0. Then the unbound intravascular silica was removed by perfusion of the mouse with MBS at 0.8 ml/min for 30 min (~24 ml). The bound silica was fixed to endothelium by perfusion with 0.1% sodium polyacrylate in MBS at 0.5 ml/min for 20 min. After 10 min, tissues were removed and homogenized as described above. The homogenates were made 60% (wt/vol) sucrose and centrifuged at 154,000 g for 30 min at 4°C

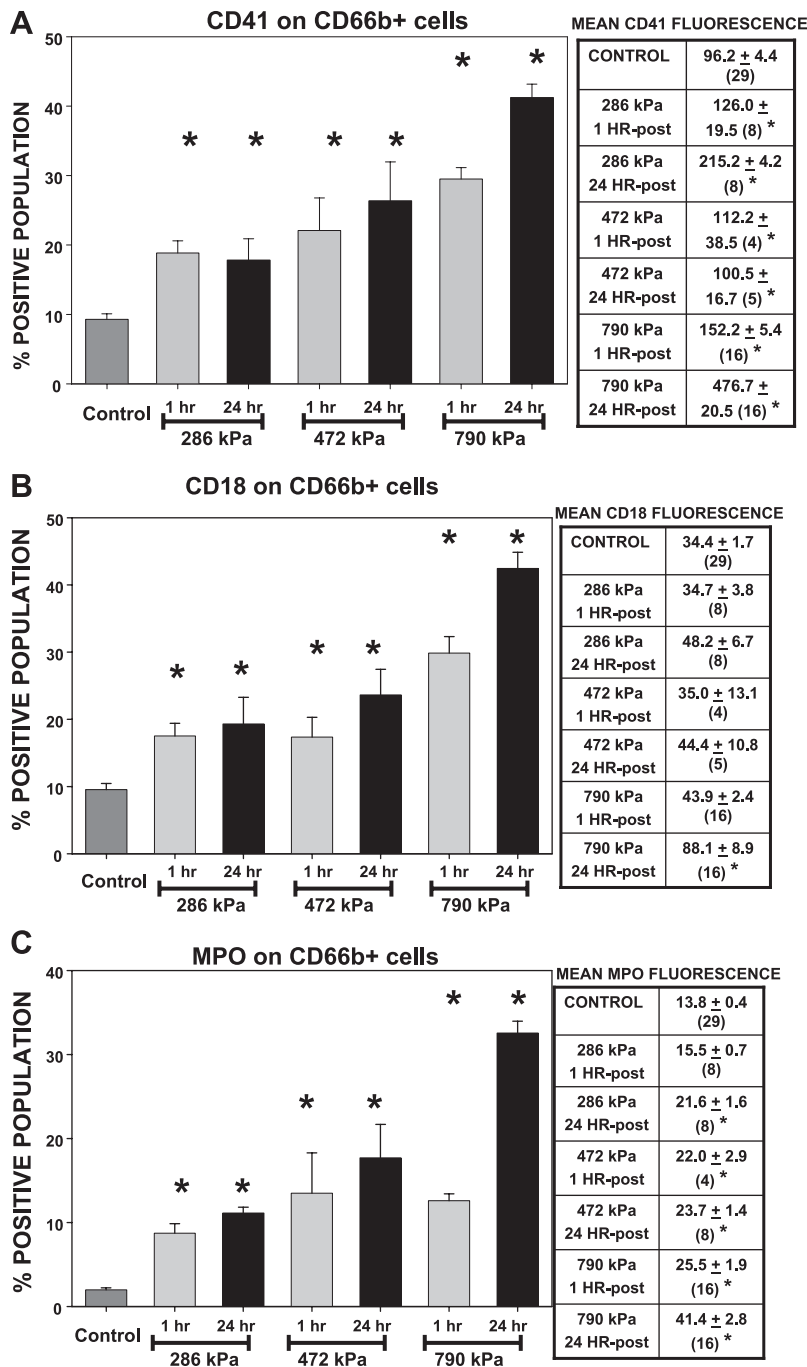


Fig. 5. Leukocyte changes with decompression. *Left*: expression of surface proteins, quantified as percentage of neutrophils with fluorescence intensity  $>10$  (%positive population), in neutrophils in blood labeled using anti-CD66b. *Right*: fluorescence per cell (mean  $\pm$  SE), as well as number of individual cell samples used for each measurement (in parentheses). \* $P < 0.05$ . A: surface expression of CD41. B: surface expression of CD18. C: surface expression of MPO.

in a swing-bucket rotor. The cell pellets were placed in 2% SDS in 50 mM Tris (pH 7.4), sonicated for 10 s, and heated at 100°C for 5 min, and the silica was removed by centrifugation at 14,000 *g* for 15 min. Supernatants were loaded onto 4–12% polyacrylamide gels, subjected to electrophoresis, and transferred to nitrocellulose paper for Western blots using  $\beta$ -actin to control for protein loading. Enrichment for endothelium assessed by comparison of caveolin-1 content with that found in standard homogenates differed among tissues, ranging from 25- to 500-fold (data not shown).

**Vascular permeability assay.** Lysine-fixable tetramethylrhodamine-conjugated dextran ( $2 \times 10^6$  Da; Invitrogen) was prepared as a 1:10 dilution of the dextran stock in MBS to yield 0.5 mg/ml. After thoracotomy, blood was removed, and the mouse was perfused with 2 ml of dextran conjugate at 0.3 ml/min and then left undisturbed for 30 min to allow dextran to diffuse into the vascular wall. Residual intravascular dextran was removed by perfusion with MBS at 0.8 ml/min for 30 min. For fixation of the dextran to tissues, the mouse was perfused with 4 ml of 1% buffered formalin at 0.3 ml/min and left in place for 10 min.

To quantify vascular permeability, perivascular dextran uptake in experimental groups was normalized to a value obtained with a control mouse included in each experiment. This was necessary because of variability in molecular weight of the individual lots of dextran. The manufacturer warns that unlabeled dextran is polydispersed and becomes even more heterogeneous during modification and purification. After intravascular formalin fixation, the procedure followed the same steps used for the cationic colloidal silica procedure. Fluorescence in the endothelium-enriched tissue homogenates was measured with a fluorescence spectrometer (555-nm excitation/580-emission) and expressed as arbitrary units per milligram of protein. If raw tissue homogenates, rather than endothelium-enriched samples, were used, the fluorescence signal was low, and no discernible difference from control was detected.

**Confocal microscopy.** Images of MPs, neutrophils, and FITC-labeled 1- $\mu$ m beads were acquired using a Zeiss Meta510 confocal microscope equipped with a Plan-Apochromat  $\times 63/1.4$  numerical aperture oil objective. FITC, RPE, and APC excitation were provided by 488-, 543-, and 644-nm laser lines, respectively, and resulting fluorescence was separated using the following band-pass filters: 500–530 nm (FITC), 560–615 nm (RPE), and 650–710 nm (APC). Pixel size was 101 nm, and pixel dwell time 1.24  $\mu$ s. Confocal pinholes were set to be one optical unit for all three channels. FITC and RPE were assigned green and red colors, respectively. The deep-red fluorophore APC was assigned the false color blue, so colocalized areas between the neutrophils and MPs were purple. The apparent sizes of the 1- $\mu$ m FITC beads were influenced by their axial positions in the confocal in-focus plane and their varying degree of mobility during the imaging acquisition time (1.24  $\mu$ s per pixel).

Images of lysine-fixable tetramethylrhodamine-conjugated dextran in tissues were prepared by sectioning organs on a vibrating microtome (20- and 50- $\mu$ m thick for brain and muscle, respectively). Tissue slices were placed on lysine-coated slides and counterstained with anti-CD66b to image neutrophils adherent to vascular walls. Slides were visualized using a confocal microscope, as previously described (30).

**Statistical analysis.** We used Sigmapstat software (Systat, Point Richmond, CA) for the statistical analysis. Neutrophil activation was analyzed by two-way ANOVA followed by the Holm-Sidak test. Single comparisons were performed using Student's *t*-tests.

## RESULTS

**MPs are elevated by decompression stress.** Mice were exposed to ambient air ( $\sim 100$  kPa, control group) or elevated partial pressures of air for 2 h, and blood samples were obtained at 1 or 24 h postdecompression. MPs were identified on the basis of size and surface expression of annexin V.

Figure 1 indicates the increase in number of MPs in blood following decompression. The cells where MPs originated were evaluated by surface expression of antigens from platelets (CD41), neutrophils (CD66b), monocytes + neutrophils (CD14), endothelial cells (CD146), and erythrocytes (GlyA). MPs exhibiting vWF (plasma protein synthesized by endothelium and megakaryocytes) were also evaluated. Total number of MPs and all MP subtypes were significantly elevated with decompression from greater pressures at 1 and 24 h (Fig. 1;  $P < 0.05$ , 2-way ANOVA).

In control and decompressed mouse MP samples, all CD41-positive MPs were also positive for CD61 as expected, given that both proteins are components of the platelet  $\alpha_2\beta_3$ -integrin. Dual-positive CD41/annexin V-expressing MPs were positive for another platelet surface marker, CD42, in  $74.1 \pm 0.9\%$  ( $n = 3$ ) of control MP samples and  $84.1 \pm 0.3\%$  ( $n = 3$ ,  $P = \text{NS}$ ) of MPs from mice 1 h after decompression from 790 kPa. There was, however, a notable difference in CD41/annexin V-expressing MPs that expressed LAMP-1. Only  $5.0 \pm 0.5\%$  ( $n = 3$ ) of MPs from control mice expressed LAMP-1, whereas  $92.9 \pm 1.0\%$  ( $n = 3$ ,  $P < 0.05$ ) of CD41/annexin V-expressing MPs from decompressed mice expressed LAMP-1.

The sum of MP subtypes shown in Fig. 1 (*bottom*) totaled  $>100\%$  in samples from mice subjected to decompression from 790 kPa, indicating that MPs interact and share antigens. To analyze this finding further, single MP samples were stained with multiple fluorescent antibodies. As shown in Fig. 2, MPs exhibiting vWF were most plentiful and concurrently expressed CD41, CD66, CD14, and CD146. Other combinations of surface markers are as shown. MP populations from mice decompressed from 790 kPa demonstrated a pattern of surface marker mixing similar to that of control mice, but the overall percentage of MPs with each surface marker combination increased significantly in mice killed at 1 and at 24 h postdecompression.

**Leukocyte activation.** Figure 3 shows a series of measurements with neutrophils, identified by CD66b expression, obtained from mice subjected to decompression from different pressures. After progressively more severe decompression,

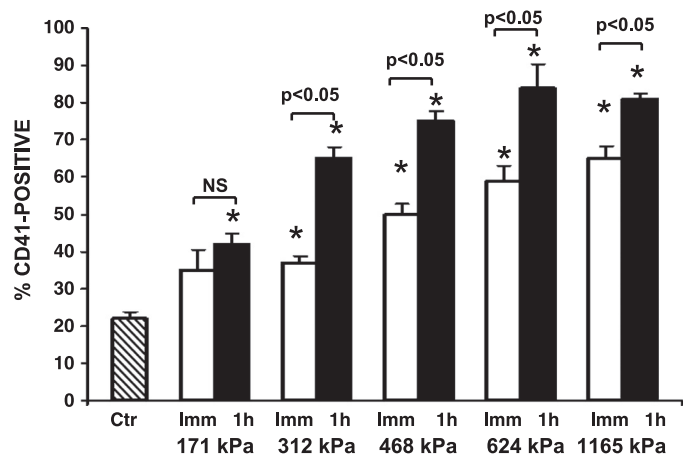


Fig. 6. Leukocyte surface expression of CD41 with decompression from varying pressures. Total leukocyte (CD18-positive cells) expression of surface CD41 is shown as percentage of cells with fluorescence intensity  $>10$  (%positive). Ctr, control. Imm, mice killed immediately after decompression; 1 h, mice killed 1 h after decompression.  $*P < 0.05$ . NS, not significant.

fluorescence intensity on the cell surface was increased for CD41, CD18 (a component of  $\beta_2$ -integrins), and MPO, with concomitantly lower fluorescence of intracellular MPO. Confocal microscopy indicated that most of the CD41-positive elements were  $<1 \mu\text{m}$  (Fig. 4), consistent with MPs or platelet fragments. Generally, maximum surface MPO staining was observed by 1 h postdecompression, except for transits from very high pressures, when further increases were noted at 24 h.

Figure 5 shows surface CD41, CD18, and MPO on neutrophils obtained from mice at 1 or 24 h postdecompression. Significantly more cells exhibited surface fluorescence for these proteins with increased pressure and time based on two-way ANOVA. Mean fluorescence per cell for each condition is also shown. CD41 was significantly different from control for all conditions, and MPO was elevated in all except the 1-h post-286 kPa samples; however, elevations in surface CD18

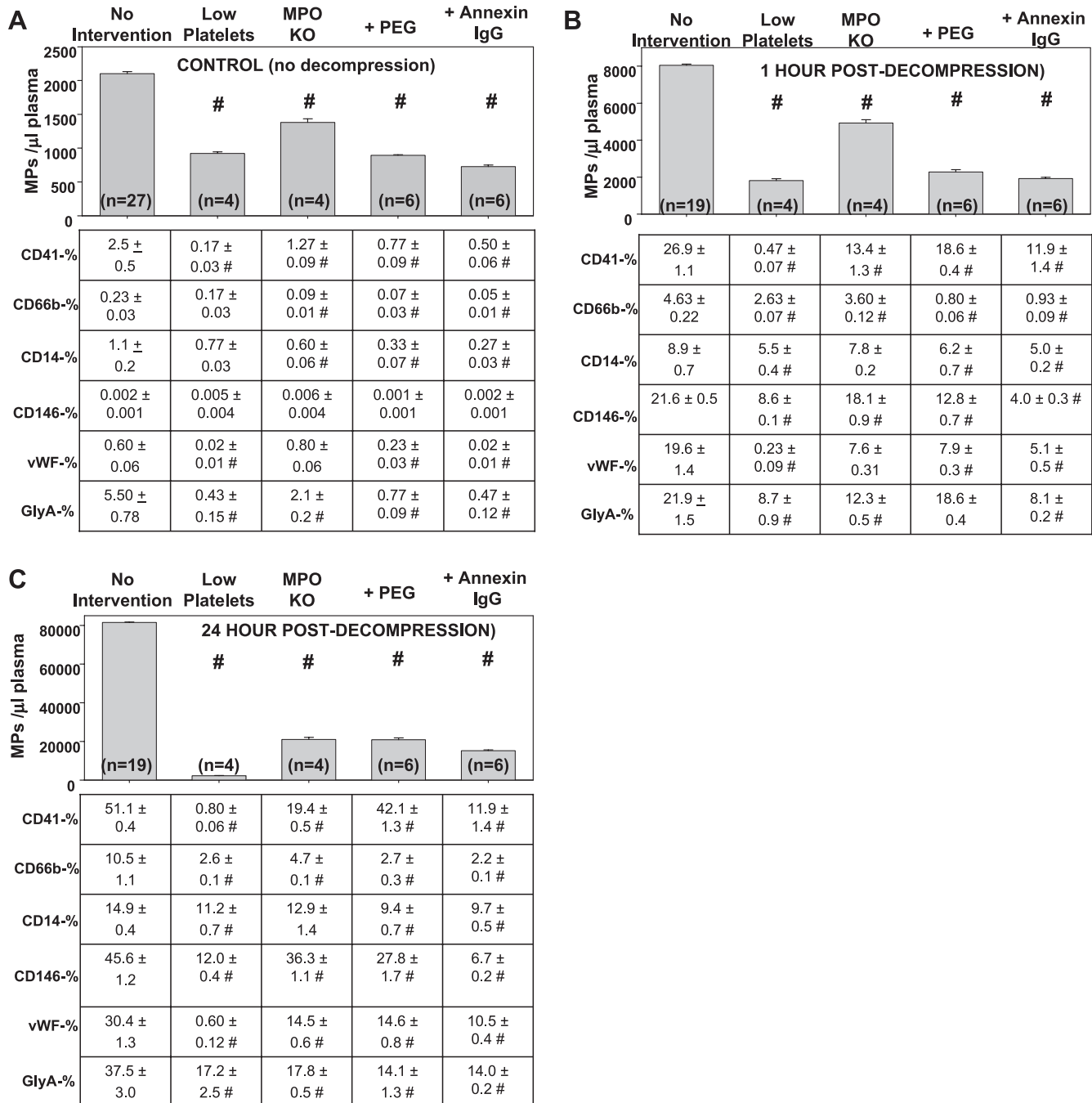


Fig. 7. Effects of various interventions on circulating MPs in blood from wild-type (“no intervention”) mice, MPO-null mice, wild-type mice treated with anti-platelet antibody (19 h prior to exposure to pressure or, in control animals, 22 h before death), wild-type mice treated with polyethylene glycol (PEG), and wild-type mice treated with antibody against annexin V (immediately after decompression or, in control animals, 24 h before death). A: data from mice that had not been subjected to decompression. B: data from mice that were killed 1 h after decompression from 790 kPa for 2 h. C: data from mice that were killed 24 h after decompression from 790 kPa. Fractions of MP populations that exhibit surface markers for various vascular cell proteins are shown in tables below histograms. #Significantly different from no intervention (by 2-way ANOVA).

were found only on cells from animals killed 24 h after decompression from the highest pressure. There were no significant changes in circulating leukocyte and platelet counts (data not shown). Decompression-induced changes were not peculiar to neutrophils, as there was a progressive elevation of CD41 on circulating leukocytes identified simply as CD18-expressing cells (Fig. 6).

Roles for platelets and MPO in MP production and neutrophil activation after decompression were investigated in thrombocytopenic and MPO-null mice. The number of circulating MPs was significantly reduced in these mice, even those not subjected to decompression, and there were commensurate changes in the subtypes of MPs (Fig. 7). Fewer MPs were found in thrombocytopenic and MPO-null mice subjected to decompression from 790 kPa and killed at 1 or 24 h postdecompression.

Changes in neutrophil surface antigen expression in thrombocytopenic and MPO-null mice are shown in Table 1. Treatment with anti-platelet antibody caused a higher fraction of neutrophils to have CD41 on the cell surface in mice not subjected to decompression, indicative of some platelet fragmentation in the circulation. Results from thrombocytopenic mice at 1 and 24 h after decompression from 790 kPa demonstrated reductions in the fraction of neutrophils expressing

CD41, as well as the mean surface fluorescence intensity of CD41, compared with cells from decompressed mice that had not been rendered thrombocytopenic. The fraction of cells expressing elevated CD18 was lower at 1 and 24 h postdecompression, although elevations in CD18 surface density were not significantly altered compared with decompressed mice that did not receive anti-platelet antibody. Thrombocytopenia resulted in lower surface MPO at 1 h postdecompression and slightly fewer cells expressing an elevation in MPO at 24 h postdecompression. Neutrophils from MPO-null mice subjected to decompression exhibited significantly lower surface fluorescence, as well as lower fractions of cells positive for CD41, MPO, and CD18, than cells from wild-type mice. Interpretations of the data are complicated, because cells from MPO-null mice that had not been subjected to decompression exhibited several differences compared with cells from wild-type mice. Notably, however, neutrophils from decompressed mice exhibited no significant elevations in values compared with those from MPO-null mice that had not been subjected to decompression stress.

*MP depletion strategies.* We hypothesized that surfactants may disperse MPs, because the integrity of their cytoskeleton is unclear, and for some cells, inhibition of cytoskeletal organization accelerates MP formation (3, 15, 16, 47). We chose to

Table 1. Surface expression of antigens on neutrophils

	No Intervention	Low Platelets	MPO-Null	PEG	Annexin-IgG
			<i>Control</i>		
CD41					
Mean	96.2 ± 4.4	45.7 ± 2.4*	88.0 ± 13.0	71.0 ± 1.7*	62.9 ± 3.4*
%	9.3 ± 0.8	17.2 ± 4.4*	5.3 ± 0.7*	5.1 ± 0.2*	8.3 ± 0.7
MPO					
Mean	13.9 ± 0.4	13.1 ± 0.7	11.9 ± 0.3*	10.8 ± 0.3*	12.1 ± 0.2
%	2.0 ± 0.2	5.3 ± 3.0	0.6 ± 0.1*	2.3 ± 0.1	2.0 ± 0.1
CD18					
Mean	34.4 ± 1.7	30.0 ± 5.3	23.3 ± 2.5*	26.4 ± 2.3*	36.8 ± 1.4
%	9.5 ± 0.9	16.5 ± 5.9	7.8 ± 2.6	5.3 ± 0.4	9.4 ± 0.7
			<i>1 h postdecompression</i>		
CD41					
Mean	152.2 ± 5.4*	58.7 ± 3.4#	58.3 ± 3.3#	155.5 ± 8.4	82.9 ± 2.8#
%	29.5 ± 1.6*	12.1 ± 0.3#	12.2 ± 0.3#	19.6 ± 1.0#	24.2 ± 1.7
MPO					
Mean	25.5 ± 1.9*	5.6 ± 0.7#	12.5 ± 0.3#	14.7 ± 0.3#	17.1 ± 1.1#
%	12.6 ± 0.8*	13.1 ± 0.2	0.6 ± 0.1#	7.7 ± 0.4#	10.3 ± 0.7
CD18					
Mean	43.9 ± 2.4	37.3 ± 1.5	24.4 ± 1.9#	23.4 ± 1.8#	33.2 ± 2.0#
%	29.9 ± 2.5*	18.2 ± 1.2#	7.1 ± 0.2#	20.6 ± 0.7#	25.4 ± 2.3
			<i>24 h postdecompression</i>		
CD41					
Mean	476.7 ± 20.5*	51.3 ± 12.1#	139.1 ± 7.2#	224.7 ± 17.2#	199.1 ± 7.9#
%	41.2 ± 1.9*	28.2 ± 5.0#	16.9 ± 4.3#	35.7 ± 3.3	24.8 ± 1.8#
MPO					
Mean	41.4 ± 2.8*	29.9 ± 5.4	13.4 ± 1.0#	23.3 ± 1.5#	23.0 ± 1.6#
%	32.6 ± 1.4*	23.9 ± 4.2#	0.6 ± 0.1#	18.6 ± 0.9#	12.2 ± 1.7#
CD18					
Mean	88.1 ± 8.9*	98.1 ± 14.4	28.7 ± 3.2#	42.5 ± 1.9#	44.2 ± 1.7#
%	42.5 ± 2.3*	28.4 ± 4.1#	10.1 ± 2.1#	36.9 ± 1.2	31.8 ± 2.6#

Values are means ± SE ( $n = 4-22$ ). Neutrophils were identified by CD66b staining, and coexpression of CD41, myeloperoxidase (MPO), and CD18 was assessed by flow cytometry. Control mice were not subjected to a decompression stress. Where indicated, mice were kept at 790 kPa for 2 h and killed 1 or 24 h later. Some mice received intraperitoneal injections with anti-platelet antiserum 24 h before experimentation to reduce platelet counts by 85–90%. MPO-null mice lacked the gene for MPO. Polyethylene glycol (PEG) and annexin V-IgG groups received the agent intravenously immediately after decompression. Injections into mice not subjected to decompression (control group) were performed 1 h before mice were killed. \* $P < 0.05$  vs. control group. # $P < 0.05$  vs. no intervention in the same animal group (1 or 24 h postdecompression).

investigate PEG telomere B, because it is known to be well tolerated, as it is an agent formerly used in clinical echocardiography trials (4, 18). Figure 8 shows the dose- and time-dependent lysis of MPs in blood obtained from decompressed mice and incubated *ex vivo*.

Figure 7 shows the reduction of MPs in control and decompressed mice injected with a 0.3% solution (wt/vol) of PEG telomere B at 0.7  $\mu\text{l/g}$  body wt *iv*. There were decreases in all subtypes of MPs with treatment. We also performed studies using a monoclonal antibody abatement strategy. Mice were injected with annexin V antibody (2  $\mu\text{g/g}$  body wt *iv*) immediately following decompression. Results were similar to PEG administration.

*MP abatement reduces intravascular neutrophil activation.* The role of MPs in neutrophil activation was examined by looking at surface expression of markers on CD66b-positive cells (Table 1). In control mice not exposed to decompression stress, injection of anti-annexin V or PEG telomere B reduced CD41 fluorescence. PEG treatment also decreased the fraction of cells positive for CD41 and mean fluorescence values for MPO and CD18. Injection with either agent immediately after mice were exposed to 790 kPa diminished most of the eleva-

tions normally observed in animals killed at 1 or 24 h postdecompression (Table 1). These agents had no significant effect on intravascular leukocyte or platelet counts (data not shown).

*Tissue neutrophil sequestration after decompression.* Confocal microscope images of tissues were examined after vascular channels had been labeled by intravenous infusion of lysine-fixable dextran. Figure 9 shows representative images of vessels in the brain and skeletal muscle of a control mouse and a mouse killed 1 h after decompression from 790 kPa. Brain sections from decompressed mice typically exhibited small ( $\leq 1\text{-}\mu\text{m}$ ) CD66b-positive particles. It appeared that intact neutrophils were adherent to skeletal muscle vessels in decompressed mice. We wished to quantify decompression-induced deposition of neutrophils or neutrophil MPs in a variety of tissues and chose to study brain, omentum, leg muscle, and psoas. Decompression caused elevations of CD66b and MPO based on a solid-phase immunoassay (Fig. 10). Cleaved caspase-3 was also probed as an apoptosis index but was not detectable.

To improve immunoassay sensitivity, tissue homogenates were enriched for vascular endothelium (1). Mice were exposed to 790 kPa for 2 h and killed at 1 or 24 h postdecompression, and endothelium-enriched homogenates were prepared from tissues. Significant elevations of CD66b, MPO, and cleaved caspase-3 were found after decompression (Table 2). The role of MPs was investigated by injection of mice with anti-annexin V or PEG telomere B immediately after decompression. PEG abrogated elevations in tissues. Antibody infusion reduced values in mice studied 24 h postdecompression, but it did not diminish MPO deposition at 1 h postdecompression in leg muscle or psoas samples.

*Increased vascular permeability associated with decompression.* Vascular permeability to rhodamine-labeled dextran was significantly elevated in all tissues at 1 and 24 h following decompression from 790 kPa (Table 3). Intravenous PEG administered immediately after decompression prevented the elevations. Intravenous anti-annexin V prevented elevations at 24 h postdecompression, but not when animals were killed at 1 h postdecompression.

## DISCUSSION

This study demonstrates that circulating MPs are elevated by decompression stress, and results provide a pathophysiological link between MPs and tissue injuries. Decompression from greater pressures results in higher MP loads from a variety of cell types. MP production is a dynamic process, because the number of MPs in the bloodstream increases for  $\geq 24$  h postdecompression. Moreover, MPs interact after they are formed, because antigenic markers from a variety of vascular cells are present on the same MPs, and this mixing is more prominent in samples at 24 h than 1 h postdecompression. Antigen sharing between MPs and vascular cells has been described, but to our knowledge, this is the first evidence of the phenomenon *in vivo* (25).

MPs have been found to play roles in a number of pathological processes (14, 19). On the basis of *ex vivo* studies, lymphocyte MPs compromise endothelial vascular reactivity, induce proinflammatory proteins, and cause oxidative stress by stimulating endothelial cell NADPH oxidase; erythrocyte MPs accelerate coagulation and adhere to endothelium; platelet-derived MPs activate neutrophils; and endothelial- and neutro-

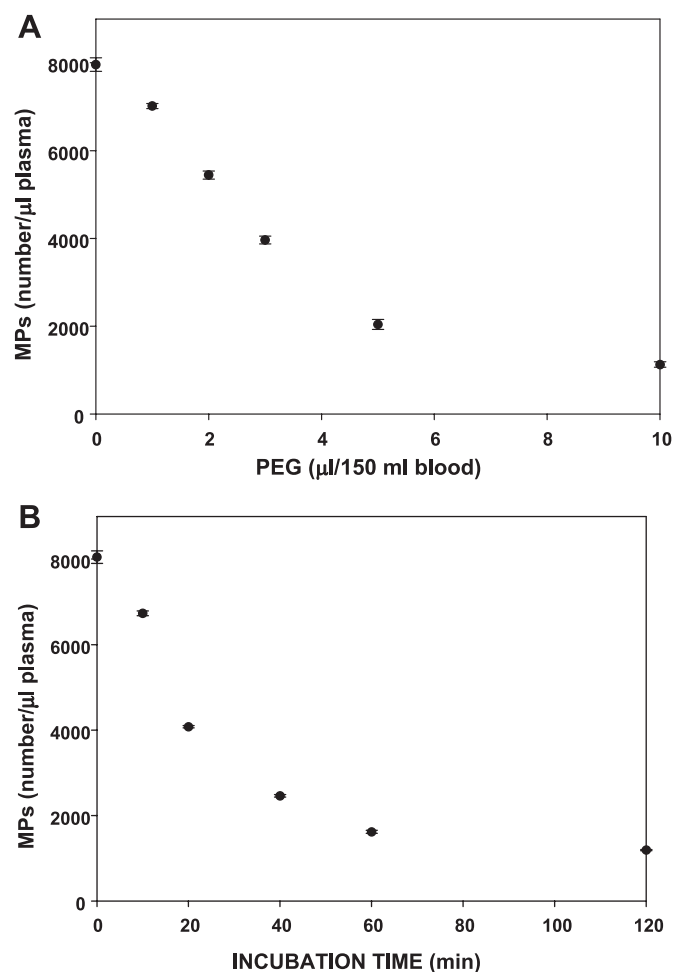


Fig. 8. MP lysis *ex vivo*. Flow cytometry was used to quantify MPs in blood from a mouse killed 1 h after decompression from 790 kPa. Values are means  $\pm$  SE ( $n = 4$ ). A: blood combined with PEG at 0–10  $\mu\text{l}/150$  ml blood and incubated at room temperature for 30 min. B: blood combined with PEG (1.2  $\mu\text{l}/100$   $\mu\text{l}$  blood) and incubated for 0–120 min at room temperature.

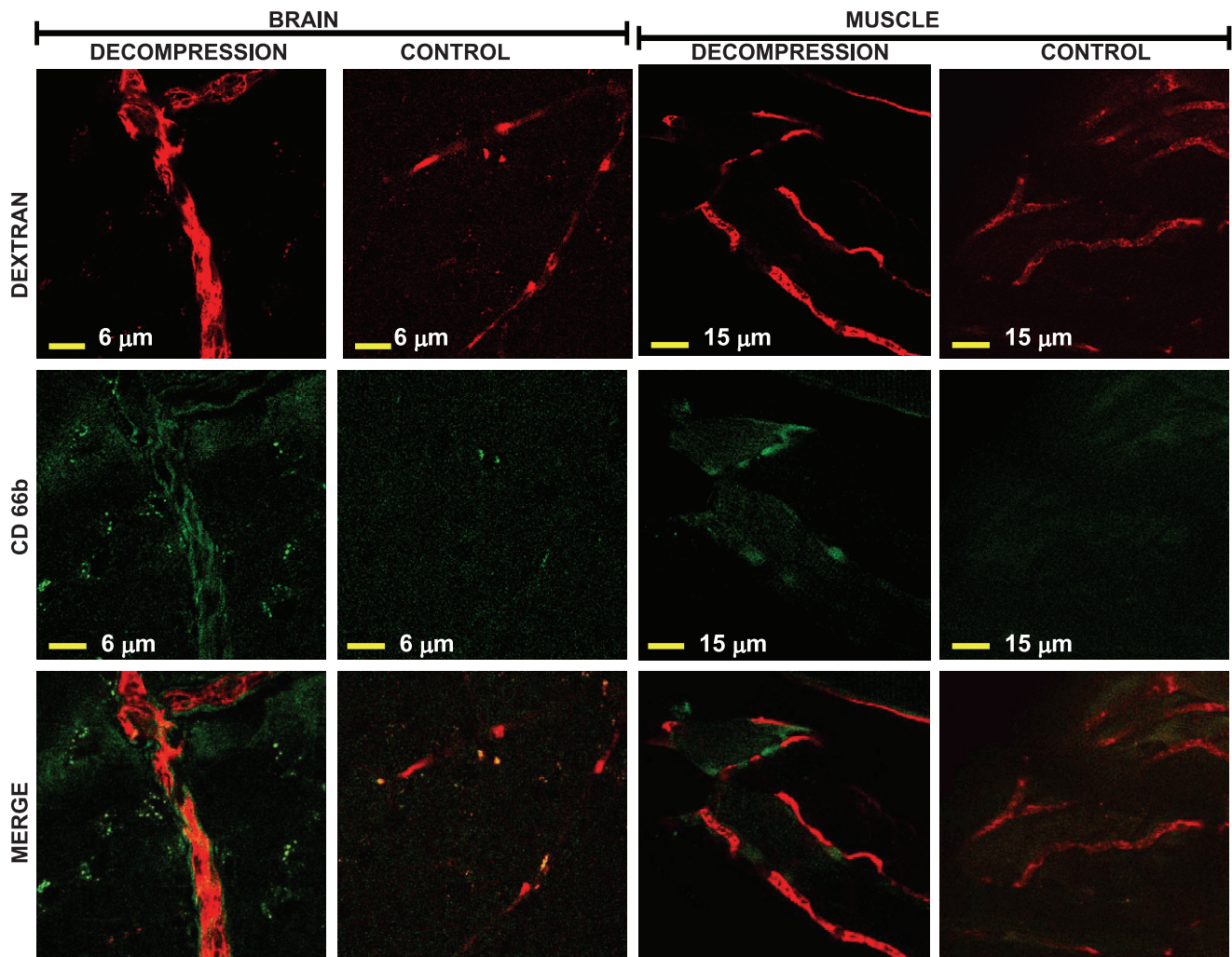


Fig. 9. Sequestration of neutrophils and dextran in vascular channels. Confocal microscope images of brain and skeletal muscle were obtained from a control mouse and a mouse killed 1 h after decompression from 790 kPa and infused with lysine-fixable rhodamine-dextran ( $2 \times 10^6$  Da) and FITC-conjugated anti-CD66b. Size of CD66b-positive particles in brain samples from decompressed mice varied, some substantially  $<1 \mu\text{m}$ ; size of CD66b-positive particles in skeletal muscle was typically consistent with the size of intact neutrophils. More intense rhodamine staining in decompressed tissues suggests a capillary leak (quantified in Table 3).

phil-derived MPs induce platelet aggregation (7, 14). Accelerated intravascular coagulation by MPs in vivo due to cancer cell-derived MPs was demonstrated using monoclonal antibodies to remove them from the circulation (42).

Our results with thrombocytopenic mice indicate that platelet-derived MPs are especially important for neutrophil activation after decompression. Over 92% of CD41/annexin V dual-positive MPs in decompressed mice express LAMP-1, whereas only 5% of MPs from control mice express this protein. Others reported LAMP-1 expression on MPs derived from activated platelets, but not on MPs derived from megakaryocytes (15). We conclude that the vast majority of MPs in control mice originate from megakaryocytes, consistent with other reports; however, activated platelets are the predominant source of CD41-positive MPs in decompressed mice. Results from MPO-null mice are consistent with data showing that MPO on the neutrophil surface can cause autoactivation (23). We conclude that neutrophil activation/degranulation following decompression involves interactions with platelet-derived MPs and that MPO adherent to the cell surface exacerbates neutrophil activation. Furthermore, as the total num-

ber of circulating MPs was lower in thrombocytopenic and MPO-null mice, it appears that neutrophil activation leads to generation of MPs from other cells, such as erythrocytes and endothelial cells.

We examined neutrophil sequestration in brain, omentum, leg muscle, and psoas. Symptoms of DCS are variable, even when individuals suffer the same decompression stresses (10, 46). Therefore, we wanted to investigate whether there may be differences in tissue responses, although MPs are expected to circulate to all organs. Brain was chosen, because among recreational scuba divers with DCS, neurological symptoms are reported in 80% of cases (17). Decompression stress induces the formation of venous gas bubbles from predominantly fatty tissue; hence, we chose to examine omentum. Our reasoning for using two different muscle types was based on differences in their dynamic properties (8). Exertion has complex effects on the propensity for bubble formation and DCS (44).

Decompression caused elevations of CD66b and MPO, and the patterns of elevations differed among the tissues. Neuro-

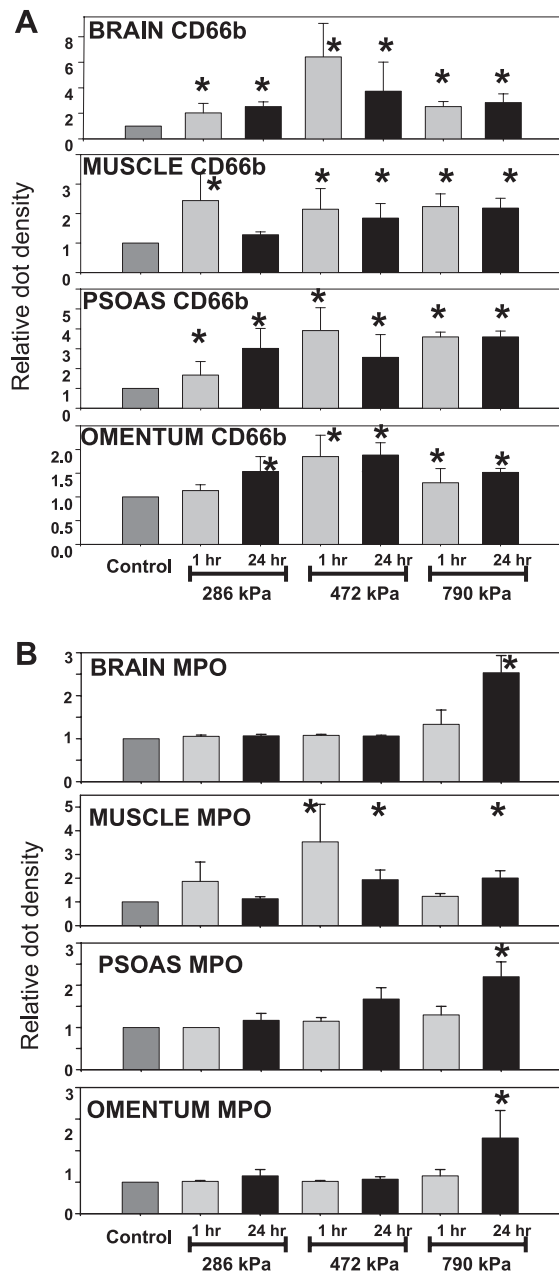


Fig. 10. Solid-phase immunoassays. Values are means  $\pm$  SE ( $n = 4$ –12 for each sample). \* $P < 0.05$ . A and B: CD66b and MPO density in tissue homogenates from control and decompressed mice.

phil MPs appear to be sequestered in the brain. We rarely found intact neutrophils adherent to brain vessels, but they were easily found in vessels of skeletal muscle. The basis for these differences requires further study. We had expected to find that the magnitude of CD66b and MPO elevations in tissues would rise in parallel. This may have failed to occur because of variable quantities of MPO in the sequestered neutrophils due to intravascular degranulation, as well as deposition of blood-borne MPO and neutrophil MPs.

We used two MP abatement strategies to examine roles for MPs in decompression stress. The *ex vivo* lytic effect of PEG on MPs prompted its use in this model. Administration of PEG or annexin V antibodies will reduce the number of circulating

Table 2. Effects of MP abatement on decompression-induced CD66b, MPO, and cleaved caspase-3 in tissues

	No Intervention ( $n = 7$ )	PEG ( $n = 4$ )	Annexin-IgG ( $n = 4$ )
<b>Brain</b>			
1 h			
CD66b	2.8 $\pm$ 0.8*	0.8 $\pm$ 0.5	0.7 $\pm$ 0.3
MPO	1.5 $\pm$ 0.1*	1.2 $\pm$ 0.3	0.8 $\pm$ 0.2
Cap-3	3.4 $\pm$ 0.8*	1.2 $\pm$ 0.6	1.5 $\pm$ 0.5
24 h			
CD66b	2.4 $\pm$ 0.4*	1.3 $\pm$ 0.4	0.9 $\pm$ 0.5
MPO	2.8 $\pm$ 0.5*	0.7 $\pm$ 0.3	1.0 $\pm$ 0.3
Cap-3	2.6 $\pm$ 0.4*	1.3 $\pm$ 0.4	1.0 $\pm$ 0.5
<b>Omentum</b>			
1 h			
CD66b	4.4 $\pm$ 1.6*	1.4 $\pm$ 0.3	0.8 $\pm$ 0.3
MPO	2.3 $\pm$ 0.5*	1.3 $\pm$ 0.4	1.3 $\pm$ 0.5
Cap-3	2.8 $\pm$ 0.7*	1.0 $\pm$ 0.1	1.2 $\pm$ 0.5
24 h			
CD66b	5.5 $\pm$ 1.8*	1.7 $\pm$ 0.6	1.0 $\pm$ 0.3
MPO	1.8 $\pm$ 0.3*	0.7 $\pm$ 0.3	0.9 $\pm$ 0.1
Cap-3	1.9 $\pm$ 0.1*	0.8 $\pm$ 0.3	1.0 $\pm$ 0.3
<b>Muscle</b>			
1 h			
CD66b	2.4 $\pm$ 0.4*	1.4 $\pm$ 0.3	0.9 $\pm$ 0.2
MPO	2.0 $\pm$ 0.3*	1.1 $\pm$ 0.4	2.2 $\pm$ 0.5*
Cap-3	2.5 $\pm$ 0.3*	1.4 $\pm$ 0.2	1.9 $\pm$ 0.6
24 h			
CD66b	2.6 $\pm$ 0.5*	1.4 $\pm$ 0.3	0.7 $\pm$ 0.1
MPO	2.5 $\pm$ 0.6*	0.7 $\pm$ 0.2	0.9 $\pm$ 0.2
Cap-3	2.9 $\pm$ 0.9*	1.1 $\pm$ 0.1	1.3 $\pm$ 0.1
<b>Psoas</b>			
1 h			
CD66b	2.4 $\pm$ 0.1*	1.4 $\pm$ 0.2	0.9 $\pm$ 0.1
MPO	2.2 $\pm$ 0.4*	1.3 $\pm$ 0.4	2.4 $\pm$ 0.4*
Cap-3	4.0 $\pm$ 0.6*	1.1 $\pm$ 0.1	1.2 $\pm$ 0.1
24 h			
CD66b	1.8 $\pm$ 0.2*	1.1 $\pm$ 0.2	0.6 $\pm$ 0.1
MPO	2.7 $\pm$ 0.5*	0.6 $\pm$ 0.3	1.7 $\pm$ 0.5
Cap-3	2.9 $\pm$ 0.6*	1.0 $\pm$ 0.1	0.9 $\pm$ 0.2

Values (means  $\pm$  SE) are expressed as ratio of Western blot band density to density of band using tissue from control animals run on the same blot (therefore, control value = 1.0). Tissue homogenates were enriched for endothelium and analyzed as described in methods. Cap-3, caspase-3. \* $P < 0.05$  vs. control.

Table 3. Effects of MP abatement on decompression-induced rhodamine-labeled dextran uptake

	No Intervention ( $n = 11$ )	PEG ( $n = 4$ )	Annexin-Ig ( $n = 4$ )
<b>Brain</b>			
1 h	1.4 $\pm$ 0.1*	1.1 $\pm$ 0.1	1.3 $\pm$ 0.1*
24 h	1.3 $\pm$ 0.1*	1.2 $\pm$ 0.4	1.0 $\pm$ 0.2
<b>Omentum</b>			
1 h	2.9 $\pm$ 0.4*	1.2 $\pm$ 0.5	1.8 $\pm$ 0.1*
24 h	1.7 $\pm$ 0.2*	1.2 $\pm$ 0.5	1.3 $\pm$ 0.4
<b>Muscle</b>			
1 h	1.8 $\pm$ 0.5*	1.2 $\pm$ 0.3	2.5 $\pm$ 0.5*
24 h	1.7 $\pm$ 0.3*	1.2 $\pm$ 0.3	1.1 $\pm$ 0.3
<b>Psoas</b>			
1 h	1.5 $\pm$ 0.2*	1.2 $\pm$ 0.2	2.6 $\pm$ 0.6*
24 h	1.5 $\pm$ 0.1*	1.1 $\pm$ 0.1	1.3 $\pm$ 0.2

Values (means  $\pm$  SE) are expressed as ratio of fluorescence/mg protein in homogenates from mice subjected to decompression from 790 kPa to fluorescence/mg in homogenates from control mice injected with the same lot of rhodamine-dextran and run on the same day. Endothelium-enriched tissue homogenates were prepared and evaluated as described in methods. \* $P < 0.05$  vs. control.

MPs, intravascular neutrophil activation, and decompression-induced tissue injuries. The antibody was not effective at limiting pathological changes in all tissues at just 1 h postdecompression. We conclude that MPs that form early after decompression are an important pathological event. Whether the marked elevation of MPs 24 h postdecompression contributes to progressive pathophysiological changes cannot be discerned from the data.

Infusion of antibody to annexin V would not be anticipated to have clinical utility and may, in fact, induce a procoagulant state (37). Use of both abatement strategies to support the pathological role for MPs was important, because surfactant agents may directly protect cells from bubble-induced membrane damage (11, 29, 39). Anti-annexin V and PEG diminished neutrophil activation after decompression (e.g., surface MPO and CD18 expression). It is intriguing that these interventions decreased the presence of CD41 on neutrophils from animals that were not subjected to decompression stress (Table 1). Blood samples were fixed immediately after phlebotomy to minimize cell activation, but we cannot definitively state whether CD41-positive MPs are normally present on the surface of leukocytes in vivo.

Tissue injury due to decompression was documented as elevations in caspase-3 and vascular permeability. A role of MPs in decompression-induced injury is supported by the inhibitory effects of the two MP abatement strategies. MPO deposition is expected to cause perivascular oxidative stress, and neutrophil proteases are also likely to compromise vascular integrity (2, 5, 38, 48). The risk for DCS rises with duration at pressure and the magnitude of depressurization. Decompression following 2 h of exposure to 171 kPa (Figs. 3 and 6) is viewed as a relatively safe “no-decompression dive.” Emphasis in this study was placed on provocative pressurizations, but it is well recognized that virtually all scuba diving will generate some intravascular bubbles and can lead to DCS. It is also important to recognize that our focus in this study was the pathophysiology of decompression stress. We did not assess functional deficits, nor did we quantify bubbles in blood or tissues, so we cannot state that our study models DCS per se.

A number of mechanisms may be responsible for MP production after decompression. Well-known processes that generate MPs include oxidative stress, cell activation/calcium influx, and apoptosis (14, 19, 36). Clearly, oxidative stress and apoptosis linked to neutrophil activation may exacerbate MP formation. This is consistent with our findings of markedly higher numbers of MPs at 24 h than at 1 h following decompression. The initial inciting event(s) for MP formation requires further investigation. On the basis of recent reports, bubble-mediated stimulation of calcium-activated big conductance potassium (BK) channels may be a central event leading to MP production (20, 21, 43).

Our results provide new insight into decompression pathophysiology and, therefore, are relevant for scuba diving, high-altitude aviation, and space exploration. Intervention with PEG, in particular, may be useful when decompression is provocative and might prove to be an effective prophylactic agent or of additive benefit with recompression in a hyperbaric chamber. The surfactant dose we used is far below the toxic dose for primates and similar to that used in clinical echocardiography trials (4, 18). Beyond their role in DCS, bubbles are an important pathological stressor in vascular surgery and any

procedure that may cause iatrogenic air embolism. MP abatement strategies may be useful in many situations when air is accidentally introduced into the circulation.

Given the pathological effects of MPs, abatement with PEG may also prove to be beneficial in conditions where MPs are elevated, such as inflammatory disorders and neoplasia (19). Because of the promiscuous exchange of surface antigens that occurs among MPs in vivo, MP abatement might be useful for improving targeted delivery of therapeutic agents when antibodies “specific” for a certain cell type are used.

#### GRANTS

This work was supported by a grant from the Office of Naval Research.

#### DISCLOSURES

No conflicts of interest, financial or otherwise, are declared by the authors.

#### REFERENCES

1. Arjunan AS, Reinartz M, Emde B, Zanger K, Schrader J. Limitations of the colloidal silica method in mapping the endothelial plasma membrane proteome of the mouse heart. *Cell Biochem Biophys* 53: 135–143, 2009.
2. Baldus S, Eiserich JP, Mani A, Castro L, Figueroa M, Chumley P, Ma W, Tousson A, White CR, Bullard DC, Brennan ML, Lusic AJ, Moore KP, Freeman BA. Endothelial transcytosis of myeloperoxidase confers specificity to vascular ECM proteins as targets of tyrosine nitration. *J Clin Invest* 108: 1759–1770, 2001.
3. Basse F, Gaffet P, Bienvenue A. Correlation between inhibition of cytoskeleton proteolysis and anti-vesiculation effect of calpeptin during A23187-induced activation of human platelets: are vesicles shed by filopod fragments? *Biochim Biophys Acta* 1190: 217–224, 1994.
4. Beppu S, Matsuda H, Shishido T, Matsumura M, Miyatake KJ. Prolonged myocardial contrast echocardiography via peripheral venous administration of QW3600 injection (EchoGen): its efficacy and side effects. *Am J Echocardiogr* 10: 11–24, 1997.
5. Brennan ML, Wu W, Fu X, Shen Z, Song W, Frost H, Vadseth C, Narine L, Lenkiewicz E, Borchers MT, Lusic AJ, Lee JJ, Lee NA, Abu-Soud HM, Ischiropoulos H, Hazen SL. A tale of two controversies: defining both the role of peroxidases in nitrotyrosine formation in vivo using eosinophil peroxidase and myeloperoxidase-deficient mice and the nature of peroxidase-generated reactive nitrogen species. *J Biol Chem* 277: 17415–17427, 2002.
6. Brubakk AO, Duplancic D, Valic Z, Palada I, Obad A, Bakovic D, Wisloff U, Dujic Z. A single air dive reduces arterial endothelial function. *J Physiol* 566: 901–906, 2005.
7. Chung SM, Bae ON, Lim KM, Noh JY, Lee MY, Jung YS, Chung JH. Lysophosphatidic acid induces thrombogenic activity through phosphatidylserine exposure and procoagulant microvesicle generation in human erythrocytes. *Arterioscler Thromb Vasc Biol* 27: 414–421, 2007.
8. Close RI. Dynamic properties of mammalian skeletal muscles. *Physiol Rev* 52: 129–197, 1972.
9. Connor DE, Exner T, Ma DD, Joseph JE. The majority of circulating platelet-derived microparticles fail to bind annexin V, lack phospholipid-dependent procoagulant activity and demonstrate greater expression of glycoprotein Ib. *Thromb Haemost* 103: 1044–1052, 2010.
10. Dembert ML, Jekel JF, Mooney LW. Health risk factors for the development of decompression sickness among US Navy divers. *Undersea Biomed Res* 11: 395–406, 1984.
11. Eckmann DM, Armstead SC, Mardini F. Surfactants reduce platelet-bubble and platelet-platelet binding induced by in vitro air embolism. *Anesthesiology* 103: 1204–1210, 2005.
12. Eftedal OS, Lydersen S, Brubakk AO. The relationship between venous gas bubbles and adverse effects of decompression after air dives. *Undersea Hyperb Med* 34: 99–105, 2007.
13. Enjeti AK, Lincz LF, Seldon M. Detection and measurement of microparticles: an evolving research tool for vascular biology. *Semin Thromb Hemost* 33: 771–779, 2007.
14. Enjeti AK, Lincz LF, Seldon M. Microparticles in health and disease. *Semin Thromb Hemost* 34: 683–692, 2008.

15. Flaumenhaft R, Dilks JR, Richardson JC, Alden E, Patel-Hett SR, Battinelli E, Klement GL, Sola-Visner M, Italiano JE. Megakaryocyte-derived microparticles: direct visualization and distinction from platelet-derived microparticles. *Blood* 113: 1112–1121, 2009.
16. Fox JEB, Austin CD, Boyles JK, Steffen PK. Role of the membrane skeleton in preventing the shedding of procoagulant-rich microvesicles from the platelet plasma membrane. *J Cell Biol* 111: 483–493, 1990.
17. Francis TJ, Pearson RR, Robertson AG, Hodgson M, Dutka AJ, Flynn ET. Central nervous system decompression sickness: latency of 1,070 human cases. *Undersea Hyperb Med* 15: 404–417, 1988.
18. Grayburn PA, Weiss JL, Hack TC, Klodas E, Raichlen JS, Vannan MA, Klein AL, Kitzman DW, Chrysant SG, Cohen JL, Abrahamson D, Foster E, Perez JE, Aurigemma GP, Panza JA, Picard MH, Byrd BF, Segar DS, Jacobson SA, Sahn DJ, DeMaria AN. Phase III multicenter trial comparing the efficacy of 2% dodecafluoropentane emulsion (EchoGen) and sonicated 5% human albumin (Albunex) as ultrasound contrast agents in patients with suboptimal echocardiograms. *J Am Coll Cardiol* 32: 230–236, 1998.
19. Hugel B, Martinez MC, Kunzelmann C, Freyssinet JM. Membrane microparticles: two sides of the coin. *Physiology* 20: 22–27, 2005.
20. Juffermans LJM, Kamp O, Dijkmans PA, Visser CA, Musters RJP. Low-intensity ultrasound-exposed microbubbles provoke local hyperpolarization of the cell membrane via activation of BK<sub>Ca</sub> channels. *Ultrasound Med Biol* 34: 502–508, 2008.
21. Juffermans LJM, Van Duk A, Jongenelen CAM, Drukarch B, Reijerkerk A, de Vries HE, Kamp O, Musters RJP. Ultrasound and microbubble-induced intra- and intercellular bioeffects in primary endothelial cells. *Ultrasound Med Biol* 35: 1917–1927, 2009.
22. Jy W, Mao WW, Horstman L, Tao J, Ahn YS. Platelet microparticles bind, activate and aggregate neutrophils in vitro. *Blood Cells Mol Dis* 21: 217–231, 1995.
23. Lau D, Mollnau H, Eiserich JP, Freeman BA, Daiber A, Gehling UM, Brummer J, Rudolph V, Munzel T, Heitzer T, Meinertz T, Baldus S. Myeloperoxidase mediates neutrophil activation by association with CD11b/CD18 integrins. *Proc Natl Acad Sci USA* 102: 431–436, 2005.
24. Lo SC, Hung CH, Lin DT, Peng HC, Huang TF. Involvement of platelet glycoprotein Ib in platelet microparticle mediated neutrophil activation. *J Biomed Sci* 13: 787–796, 2006.
25. Mack M, Kleinschmidt A, Bruhl H, Klier C, Nelson PJ, Cihak J, Plachy J, Stangassinger M, Erfle V, Schlondorff D. Transfer of the chemokine receptor CCR5 between cells by membrane-derived microparticles: a mechanism for cellular human immunodeficiency virus 1 infection. *Nat Med* 6: 769–775, 2000.
26. Madden LA, Christmas BC, Mellor D, Vince RV, Midgley AW, McNaughton LR, Atkins SL, Laden G. Endothelial function and stress response after simulated dives to 10 msw breathing air or oxygen. *Aviat Space Environ Med* 81: 41–51, 2010.
27. Martin JD, Thom SR. Vascular leukocyte sequestration in decompression sickness and prophylactic hyperbaric oxygen therapy in rats. *Aviat Space Environ Med* 73: 565–569, 2002.
28. Mesri M, Altieru DC. Leukocyte microparticles stimulate endothelial cell cytokine release and tissue factor induction in a JNK1 signaling pathway. *J Biol Chem* 274: 23111–23118, 1999.
29. Michaels JD, Petersen JF, McIntire LV, Papoutsakis ET. Protection mechanisms of freely suspended animal cells (CRL 8018) from fluid-mechanical injury. Viscometric and bioreactor studies using serum, Pluronic F68 and polyethylene glycol. *Biotechnol Bioeng* 38: 169–180, 1991.
30. Milovanova T, Bhopale VM, Sorokina EM, Moore JS, Hunt TK, Velazquez OC, Thom SR. Lactate stimulates vasculogenic stem cells via the thioredoxin system and engages an autocrine activation loop involving hypoxia inducible factor-1. *Mol Biol Cell* 28: 6248–6261, 2008.
31. Nossum V, Hjelde A, Brubakk AO. Small amounts of venous gas embolism cause delayed impairment of endothelial function and increase polymorphonuclear neutrophil infiltration. *Eur J Appl Physiol* 86: 209–214, 2002.
32. Nossum V, Koteng S, Brubakk AO. Endothelial damage by bubbles in the pulmonary artery of the pig. *Undersea Hyperb Med* 26: 1–8, 1999.
33. Olszanski R, Radziwon P, Baj Z, Kaczmarek P, Giedrojc J, Galar M, Kloczko J. Changes in the extrinsic and intrinsic coagulation pathways in humans after decompression following saturation diving. *Blood Coagul Fibrinolysis* 12: 269–274, 2001.
34. Philp RB, Ackles KN, Inwood MJ, Livingstone SD, Achimastos A, Binns-Smith M, Radomski MW. Changes in the hemostatic system and in blood and urine chemistry of human subjects following decompression from a hyperbaric environment. *Aerosp Med* 43: 498–505, 1972.
36. Pirro M, Schillaci G, Bagaglia F, Menecali C, Paltriccia R, Mannarino MR, Capanni M, Velardi A, Mannarino E. Microparticles derived from endothelial progenitor cells in patients at different cardiovascular risk. *Atherosclerosis* 197: 757–767, 2008.
37. Schutters K, Reutelingsperger C. Phosphatidylserine targeting for diagnosis and treatment of human diseases. *Apoptosis* 15: 1072–1082, 2010.
38. Sohn HY, Krotz F, Zahler S, Gloe T, Keller M, Theisen K, Schiele TM, Klauss V, Pohl U. Crucial role of local peroxynitrite formation in neutrophil-induced endothelial cell activation. *Cardiovasc Res* 57: 804–815, 2003.
39. Swim HE, Parker RF. Effect of pluronic F68 on growth fibroblasts in suspension on rotary shaker. *Proc Soc Exp Biol Med* 103: 252–254, 1960.
40. Thom SR, Bhopale VM, Han ST, Clark JM, Hardy KR. Intravascular neutrophil activation due to carbon monoxide poisoning. *Am J Respir Crit Care Med* 174: 1239–1248, 2006.
41. Thom SR, Mendiguren I, Van Winkle T, Fisher D, Fisher AB. Smoke inhalation with a concurrent systemic stress results in lung alveolar injury. *Am J Respir Crit Care Med* 149: 220–226, 1994.
42. Thomas GM, Panicot-Dubois L, Lacroix R, Dignat-George F, Lombardo D, Dubois C. Cancer cell-derived microparticles bearing P-selectin glycoprotein ligand 1 accelerate thrombus formation in vivo. *J Exp Med* 206: 1913–1927, 2009.
43. Tran TA, Guennec YL, Bougnoux P, Tranquart F, Bouakaz A. Characterization of cell membrane response to ultrasound activated microbubbles. *IEEE Trans Ultrason Ferroelectr Freq Control* 55: 44–49, 2008.
44. Vann RD. Mechanisms and risk of decompression. In: *Bove and Davis' Diving Medicine* (4th ed.), edited by Bove AA. Philadelphia: Saunders, 2004, p. 127–183.
45. Vince RV, McNaughton LR, Taylor L, Midgley AW, Laden G, Madden LA. Release of VCAM-1 associated endothelial microparticles following simulated SCUBA dives. *Eur J Appl Physiol* 105: 507–513, 2009.
46. Weathersby PK, Homer LD, Flynn ET. On the likelihood of decompression sickness. *J Appl Physiol* 57: 815–825, 1984.
47. Yano Y, Kambayashi J, Shiba E, Sakon M, Oiki E, Fukuda K, Kawasaki T, Mori T. The role of protein phosphorylation and cytoskeletal reorganization in microparticle formation from the platelet plasma membrane. *Biochem J* 299: 303–308, 1994.
48. Zhang R, Brennan ML, Shen Z, MacPherson JC, Schmitt D, Molenda CE, Hazen SL. Myeloperoxidase functions as a major enzymatic catalyst for initiation of lipid peroxidation at sites of inflammation. *J Biol Chem* 277: 46116–46122, 2002.